Nonlinear Dynamics and Systems Theory, **21** (3) (2021) 262–279

DTC-SVM Sensorless Control of Five-Phase Induction Motor Based on Two Different Rotor Speed Estimation Approaches

B. S. Khaldi [1,2,*], A. Kouzou [1], M. O. Mahmoudi [2] and D. Boukhetala [2]

[1] *Laboratory of Applied Automation and Industrial Diagnosis, Faculty of Sciences and Technology, Djelfa University, Algeria.*
[2] *Process Control Laboratory, National Polytechnic School, Algiers, Algeria.*

Received: March 9, 2021; Revised: May 20, 2021

Abstract: This paper deals with the study and analysis of the five-phase induction motor (FFIM) sensorless control based on the combination of the direct torque control (DTC) technique and the space vector modulation (SVM) technique. Indeed, this sensorless control applied to the FFIM is achieved using two different rotor speed estimation approaches. The first approach is based on the adaptive flux and speed observer for ensuring the estimation of the rotor speed and rotor flux at once. The second approach is performed based on the model reference adaptive system estimator for ensuring the estimation of the rotor speed. The applications of both estimation approaches with the combined techniques for ensuring the sensorless control of the FFIM are presented and analyzed to shed light on their main performances compared with each other based on the main predominant constraints such as the processor computation time and memory size costs, robustness against the machine parameter variation and the accuracy of estimation. The analysis of the results obtained by simulation allows the validation of both approaches in ensuring the sensorless control of the FFIM using the DTC-SVM with some limited differences.

Keywords: *direct torque control (DTC); space vector modulation (SVM); stator flux oriented control (SFOC); five-phase induction machine (FFIM); speed sensorless; adaptive observer; model reference adaptive system (MRAS).*

Mathematics Subject Classification (2010): 03B52, 93C42, 94D05.

* Corresponding author: mailto:bs.khaldi@gmail.com

1 Introduction

Multiphase drives have recently gained interest due to their advantages over traditional three-phase drives for high-power applications (e.g., locomotive traction, electric ship propulsion) and/or high-current applications (e.g., electric and hybrid vehicles). Indeed, there are plenty benefits of a greater number of phases such as reducing the inverter per leg power, decreasing the amplitude of torque pulsations in motor drives and lowering the dc-link current harmonics [1]. Another very interesting feature of this kind of machines is their capability to start-up and run even with one or two non-adjacent stator phases under open or short circuit. Hence, it provides high reliability, especially in industrial applications where the stop of the machine has to be avoided during working process.

The technique of torque control of induction motors was developed and presented by I. Takahashi as a direct torque control (DTC) [2], and by M. Depenbrock as a direct self control (DSC) [3]. It is possible to enhance the operating characteristics of not only the motor but also the voltage source inverter (VSI) supplying such drives by using the direct control of the stator flux and torque instead of the traditional current control technique.

The basic principle behind a three-phase ac drive's DTC is to directly and independently control the electromagnetic torque and flux linkage by using six or eight voltage space vectors saved in a lookup table. Since the DTC approach has additional advantages when applied to multiphase machines, in recent years the application of the DTC technique for multiphase machines has received a widespread attention [4–6]. The five-phase induction motor direct torque control can minimize successfully the ripple amplitude of both the stator flux and the torque, allowing a more reliable flux and torque control [7].

The use of the space vector modulation (SVM) retains the transient performance and robustness of the DTC, and decreases the torque ripple of the steady state. At the same time, the switching frequency can also be kept constant and controllable [8]. It can be said that the five-phase inverter can give more flexibility due to its ability to provide 32 space vector voltages, hence the elaboration of the desired torque and flux can be obtained in a more flexible and accurate way compared to its counter-part of three phases.

A large number of studies have been carried out focusing mainly on sensorless drives on a three-phase induction machine to increase the efficiency and reduce cost. Although the cases of the sensorless control of a multiphase motor drive are limited in the literature, nevertheless few documented research activities treat the sensorless control of a five-phase motor as a three-phase case extension. B. S. Khaldi et al. [9] have presented a comparison between a new sensorless method and an adaptive observer for the DTC applied on the five-phase IM. H. Echeikh et al. [10] have proposed an improved sliding mode observer for the sensorless control of a five-phase induction motor. O. Gonzalez et al. [11] have proposed a speed sensorless control of a five-phase induction machine by using an inner loop of the model-based predictive control. In [12], the authors have described the use of 02 speed observers system planes for a five-phase machine supplied by the current source inverter.

It is known that the most popular speed sensorless control is the MRAS technique because of its simple implementation. In some previous works, the MRAS speed estimator is applied for the five-phase induction machine with several schemes such as the scalar control [13], the vector control [14], and the SVM-backstepping control [15]. However, a limited number of works have investigated the direct torque control of a five-phase induction machine.

In this paper, the authors present an extension of the application of the MRAS technique for a three-phase machine to be incorporated with the application of the DTC for a five-phase induction motor for ensuring its sensorless control and compare it with a speed and flux full-order adaptive observer which is used for the same purpose.

The following part of this paper is organized in five sections. Section 2 focuses on the presentation of the modeling of a five-phase induction machine; Section 3 describes in details the direct torque control of a five-phase induction motor and the space vector PWM. In Section 4, the authors present the first observer used for the estimation of the rotor speed and the rotor flux called a speed and flux full-order adaptive observer. Further, in Section 5, the extended application of the MRAS to a five-phase induction motor is presented. Section 6 is dedicated to the results obtained via simulation. This paper ends with a conclusion.

2 Modeling of a Five-Phase Induction Machine

In the present paper, the modeling of the five-phase induction machine will be based on some simplifying hypotheses, which can be presented as follows:

- The motor has an unsaturated symmetrical armature.
- The hysteresis and eddy currents are negligible.
- The air gap is of uniform thickness, the slotting effect is neglected.
- The proper and mutual inductances are independent of the currents flowing in the different windings.
- The distribution of the flux along the air gap is assumed to be a sine waveform.
- The skin effect is negligible.
- Considering regular phase shifting between each two sequenced phases, the windings in all phases are supposed to be identical.

The model of the machine is presented in a common reference frame, rotating at an arbitrary angular speed as shown in Fig.1.

The model of the five-phase squirrel cage induction machine can be written in matrix form as follows [16]:

$$\begin{cases} [V^s_{abcde}] = [R_s]\,[I^s_{abcde}] + \frac{d}{dt}\,[\phi^s_{abcde}], \\ [V^r_{abcde}] = [R_r]\,[I^r_{abcde}] + \frac{d}{dt}\,[\phi^r_{abcde}] = 0, \end{cases} \tag{1}$$

$$\begin{cases} [\phi^s_{abcde}] = [L_s]\,[I^s_{abcde}] + [L_{sr}]\,[I^r_{abcde}], \\ [\phi^r_{abcde}] = [L_r]\,[I^r_{abcde}] + [L_{rs}]\,[I^s_{abcde}]\,, \end{cases} \tag{2}$$

where

$$\begin{bmatrix} V^s_{abcde} \\ V^r_{abcde} \end{bmatrix} = \begin{bmatrix} V^s_a & V^s_b & V^s_c & V^s_d & V^s_e \\ V^r_a & V^r_b & V^r_c & V^r_d & V^r_e \end{bmatrix}^T, \tag{3}$$

$$\begin{bmatrix} I^s_{abcde} \\ I^r_{abcde} \end{bmatrix} = \begin{bmatrix} I^s_a & I^s_b & I^s_c & I^s_d & I^s_e \\ I^r_a & I^r_b & I^r_c & I^r_d & I^r_e \end{bmatrix}^T, \tag{4}$$

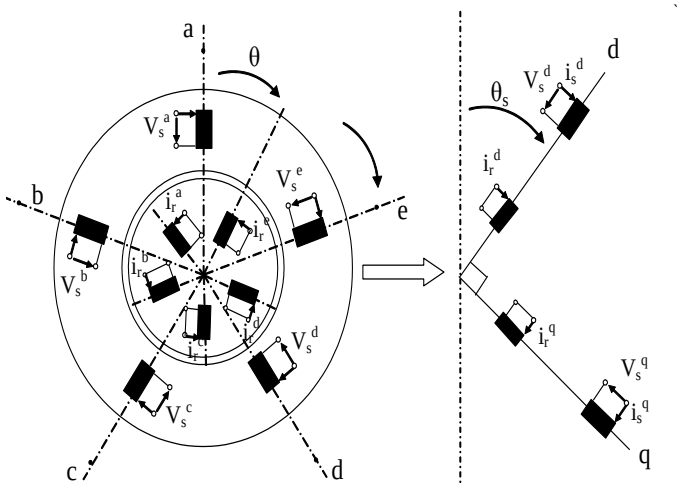

Figure 1: Park transformation applied to the five-phase induction machine.

$$\begin{bmatrix} \phi^s_{abcde} \\ \phi^r_{abcde} \end{bmatrix} = \begin{bmatrix} \phi^s_a & \phi^s_b & \phi^s_c & \phi^s_d & \phi^s_e \\ \phi^r_a & \phi^r_b & \phi^r_c & \phi^r_d & \phi^r_e \end{bmatrix}^T. \tag{5}$$

For the simplification of the model of the machine under study, which is presented in the natural frame abc, the following matrices of transformation are used for the stator and the rotor to obtain the model of the machine in biphase frames while keeping the power invariant. These matrices are presented as follows:

$$A_s = \sqrt{\frac{2}{5}} \begin{bmatrix} \cos\theta_s & \cos(\theta_s - \alpha) & \cos(\theta_s - 2\alpha) & \cos(\theta_s + 2\alpha) & \cos(\theta_s + \alpha) \\ -\sin\theta_s & -\sin(\theta_s - \alpha) & -\sin(\theta_s - 2\alpha) & -\sin(\theta_s + 2\alpha) & -\sin(\theta_s + \alpha) \\ 1 & \cos(2\alpha) & \cos(4\alpha) & \cos(4\alpha) & \cos(2\alpha) \\ 0 & \sin(2\alpha) & \sin(4\alpha) & -\sin(4\alpha) & -\sin(2\alpha) \\ 1/\sqrt{2} & 1/\sqrt{2} & 1/\sqrt{2} & 1/\sqrt{2} & 1/\sqrt{2} \end{bmatrix}, \tag{6}$$

$$A_r = \sqrt{\frac{2}{5}} \begin{bmatrix} \cos\beta & \cos(\beta - \alpha) & \cos(\beta - 2\alpha) & \cos(\beta + 2\alpha) & \cos(\beta + \alpha) \\ -\sin\beta & -\sin(\beta - \alpha) & -\sin(\beta - 2\alpha) & -\sin(\beta + 2\alpha) & -\sin(\beta + \alpha) \\ 1 & \cos(2\alpha) & \cos(4\alpha) & \cos(4\alpha) & \cos(2\alpha) \\ 0 & \sin(2\alpha) & \sin(4\alpha) & -\sin(4\alpha) & -\sin(2\alpha) \\ 1/\sqrt{2} & 1/\sqrt{2} & 1/\sqrt{2} & 1/\sqrt{2} & 1/\sqrt{2} \end{bmatrix}. \tag{7}$$

Here

$$\theta_s = \int \omega_a dt \text{ and } \beta = \theta_s - \theta = \int (\omega_a - \omega)\, dt, \tag{8}$$

where $\alpha = 2\pi/5$, β is the instantaneous angular position of the d-axis of the common reference frame, ω_a is the arbitrary speed of the selected common reference frame, ω is the rotor angular (electrical) speed and θ is the instantaneous rotor position. Using these transformations, the equations in the $d - q - d_1 - q_1 - 0$ domain can be written as

$$\left[V^s_{dqd_1q_10}\right] = [A_s]\,[V^s_{abcde}], \quad \left[\phi^r_{dqd_1q_10}\right] = [A_r]\,[\phi^r_{abcde}], \tag{9}$$

$$\left[V^r_{dqd_1q_10}\right] = [A_r]\left[V^r_{abcde}\right], \quad \left[I^s_{dqd_1q_10}\right] = [A_s]\left[I^s_{abcde}\right], \tag{10}$$

$$\left[\phi^s_{dqd_1q_10}\right] = [A_s]\left[\phi^s_{abcde}\right], \quad \left[I^r_{dqd_1q_10}\right] = [A_r]\left[I^r_{abcde}\right]. \tag{11}$$

The stator and rotor voltage equations for the machine in arbitrary reference frame can be written as (the symbol p stands for d/dt)

$$\begin{cases} V_{ds} = R_s I_{ds} - \omega_a \phi_{qs} + p\phi_{ds}, & V_{d_1 s} = R_s I_{d_1 s} + p\phi_{d_1 s}, \\ V_{qs} = R_s I_{qs} + \omega_a \phi_{ds} + p\phi_{qs}, & V_{q_1 s} = R_s I_{q_1 s} + p\phi_{q_1 s}, \\ V_{dr} = R_r I_{dr} - (\omega_a - \omega)\,\phi_{qr} + p\phi_{dr}, & V_{d_1 r} = R_r I_{d_1 r} + p\phi_{d_1 r}, \\ V_{qr} = R_r I_{qr} + (\omega_a - \omega)\,\phi_{dr} + p\phi_{qr}, & V_{q_1 r} = R_r I_{q_1 r} + p\phi_{q_1 r}. \\ V_{0s} = R_s I_{0s} + p\phi_{0s}, & V_{0r} = R_r I_{0r} + p\phi_{0r}. \end{cases} \tag{12}$$

The flux linkages ϕ_{ds}, ϕ_{qs}, ϕ_{dr} and ϕ_{qr} can be written after transformation as

$$\begin{cases} \phi_{ds} = (L_{ls} + L_m)\, I_{ds} + L_m I_{dr}, & \phi_{d_1 s} = L_{ls} I_{d_1 s}, \\ \phi_{qs} = (L_{ls} + L_m)\, I_{qs} + L_m I_{qr}, & \phi_{q_1 s} = L_{ls} I_{q_1 s}, \\ \phi_{dr} = (L_{lr} + L_m)\, I_{dr} + L_m I_{ds}, & \phi_{d_1 r} = L_{lr} I_{d_1 r}, \\ \phi_{qr} = (L_{lr} + L_m)\, I_{qr} + L_m I_{qs}, & \phi_{q_1 r} = L_{lr} I_{q_1 r}. \\ \phi_{0s} = L_{ls} I_{0s}, & \phi_{0r} = L_{lr} I_{0r}. \end{cases} \tag{13}$$

In the stationary reference frame, the stator and rotor equations of the five-phase IM can also be obtained as follows:

$$\begin{cases} V_{\alpha s} = R_s I_{\alpha s} + p\phi_{\alpha s}, & V_{d_1 s} = R_s I_{d_1 s} + p\phi_{d_1 s}, \\ V_{\beta s} = R_s I_{\beta s} + p\phi_{\beta s}, & V_{q_1 s} = R_s I_{q_1 s} + p\phi_{q_1 s}, \\ V_{0s} = R_s I_{0s} + p\phi_{0s}, & \\ V_{\alpha r} = R_r I_{\alpha r} + \omega\phi_{\beta r} + p\phi_{\alpha r}, & V_{d_1 r} = R_r I_{d_1 r} + p\phi_{d_1 r}, \\ V_{\beta r} = R_r I_{\beta r} - \omega\phi_{\alpha r} + p\phi_{\beta r}, & V_{q_1 r} = R_r I_{q_1 r} + p\phi_{q_1 r}, \\ V_{0r} = R_r I_{0r} + p\phi_{0r}, & \end{cases} \tag{14}$$

$$\begin{cases} \phi_{\alpha s} = (L_{ls} + L_m)\, I_{\alpha s} + L_m I_{\alpha r}, & \phi_{d_1 s} = L_{ls} I_{d_1 s}, \\ \phi_{\beta s} = (L_{ls} + L_m)\, I_{\beta s} + L_m I_{\beta r}, & \phi_{q_1 s} = L_{ls} I_{q_1 s}, \\ \phi_{\alpha r} = (L_{lr} + L_m)\, I_{\alpha r} + L_m I_{\alpha s}, & \phi_{d_1 r} = L_{lr} I_{d_1 r}, \\ \phi_{\beta r} = (L_{lr} + L_m)\, I_{\beta r} + L_m I_{\beta s}, & \phi_{q_1 r} = L_{lr} I_{q_1 r}, \\ \phi_{0r} = L_{lr} I_{0r}, & \phi_{0s} = L_{ls} I_{0s}. \end{cases} \tag{15}$$

The torque equation can be written as

$$T_e = P L_m \left(I_{dr} I_{qs} - I_{ds} I_{qr}\right). \tag{16}$$

Therefore, the difference between the model of the five-phase machine and the model of the three-phase machine is the existence of $d_1 - q_1$ components in (12)-(15).From equations (12) and (13), it is clear that the components of the rotor and stator in the $d_1 - q_1$ frame are completely decoupled from the components of $d - q$ and one from each other. On the other side, the rotor and stator components in $d_1 - q_1$ are totally decoupled, hence these components do not contribute to the production of the flux or the electromagnetic couple, however they can produce more losses in the machine. Due to the short-circuited rotor winding and star connection of the stator winding, it is supposed further that the five-phase components are balanced in the stator and rotor, the zero sequence components of both the stator and the rotor can be omitted from further consideration.

This means that the five-phase induction machine model would be identical to the three-phase induction machine model. Therefore, as with a three-phase induction machine, the same DTC concepts can be used.

3 Direct Torque Control of a Five-Phase Induction Motor

The direct torque control approach was found to be a powerfull technique for ensuring a quick dynamic response in the three-phase induction motor, hence it is expected to achieve the same features when applied to the five-phase induction motor which is presented in this section. The DTC approach is based on the vector theory of space voltage [2, 3]. The decoupling of the flux and the torque can be accomplished based on the merits of the used five-phase inverters, which allows obtaining of suitable space voltage vectors among the available switching patterns offered by this kind of inverter.

The DTC control technique was demonstrated in several previous works to be more simple compared to the conventional control techniques such as the field-oriented control, which have been used intensively for the control of many machine topologies. Indeed, the DTC does not use the current controller and PWM signal generators, in contrast, the torque response is greatly improved [17], which makes this technique more attractive to be applied within many topologies of electrical motors such as multi-phase machines.

The five-phase motor is fed by a five-phase voltage source inverter as shown in Fig.2. In this kind of inverter, 32 switching states can be obtained, there are two zero voltage states associated with either, all upper switches are "on" or all bottom switches are "off". At the same time, there are thirty non-zero active vectors, which are distributed in three concentrated regular decagons, where these active vectors are presenting the difference vertices. The difference between the three decagons is the length of their vertices with constant rations referring to the inner decagon vertices that can be defined as the golden ratio ϕ, $1 : 1.618 : 1.618^2$ (Fig.3).

The SV-PWM is used to produce almost the best sinusoidal phase output voltages, where the most low frequency dominant harmonics have neglected amplitude compared to the fundamental component. In this paper, it is proposed to use only the active vectors, which are located in the two outer decagons presenting the large and medium active vectors. In each switching period, the use of two adjacent medium space vectors with two large active space vectors makes it possible to maintain a zero average value [18], and consequently, providing almost sinusoidal output.

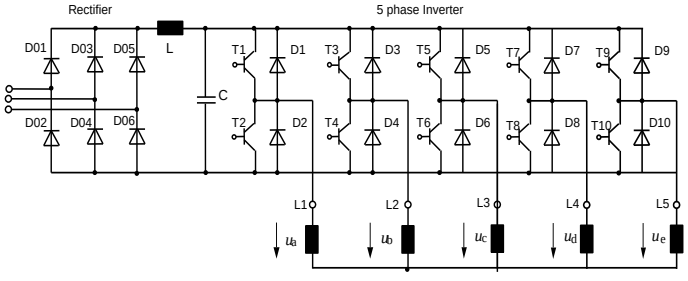

Figure 2: Five-phase pulsewidth-modulation inverter.

The stator vector control or the stator flux oriented control (SFOC) is applied to the five-phase induction machine. It is based basically on two types of estimators, which are used to ensure the estimation in real time of the stator flux and the rotor speed. The first one is the adaptative flux and speed observer, and the second one is the MRAS estimator. The principal of the SFOC presented in this paper is illustrated in Fig.4, where

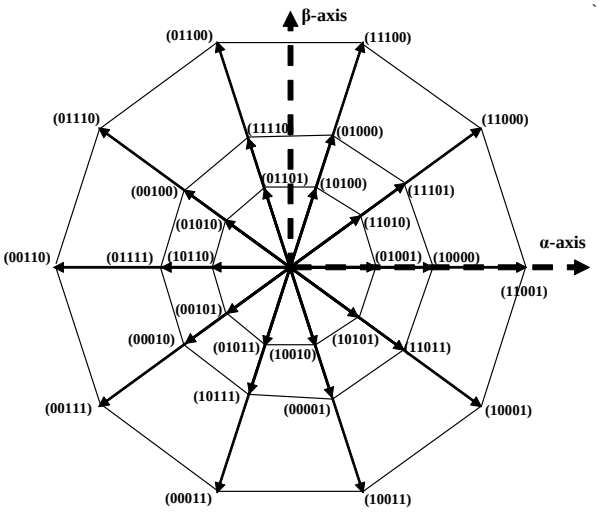

Figure 3: Thirty non-zero switching vectors for the five-phase IM motor drive in the $\alpha - \beta$ plane.

the control can be achieved based on the use of one of the aforementioned estimators as it is indicated in Fig.4.

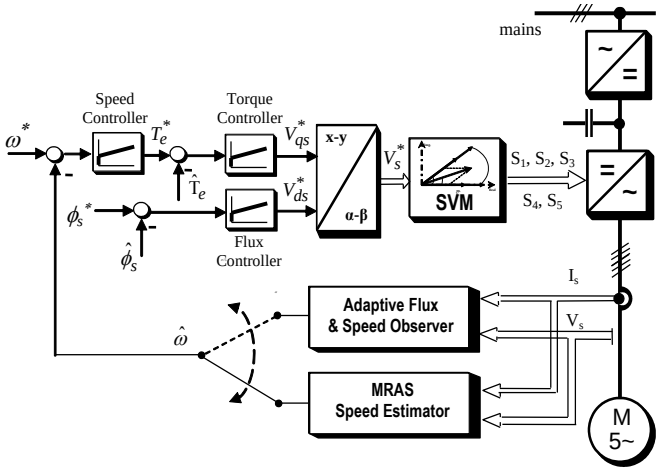

Figure 4: Schematic block diagram of the speed sensorless five-phase induction motor.

The mechanical equation of the motor can be expressed as follows:

$$\begin{cases} \frac{J}{P}\frac{d\omega}{dt} = T_e - T_L - \frac{T_f}{P}\omega, \\ T_e = P\left(\phi_{ds} I_{qs} - \phi_{qs} I_{ds}\right), \end{cases} \tag{17}$$

where T_e is the electromagnetic torque developed by the motor in (N.m), T_L is the load torque in (N.m), T_f is the friction torque in (N.m) and ω is the rotor speed in rad/s.

The voltage stator equation presented in equation (12) can be rewritten in the stator flux coordinate, where the stator linkage flux is aligned with the d axis, which means that the q component will be equal to zero ($\phi_{ds} = \phi_s$, $\phi_{qs} = 0$). Hence, the voltage stator equations become as follows:

$$\begin{cases} V_{ds} = R_s I_{ds} + \frac{d\phi_s}{dt}, \\ V_{qs} = R_s I_{qs} + \omega_a \phi_s, \\ T_e = p\phi_s I_{qs}. \end{cases} \tag{18}$$

From (18), the motor can be expressed as follows:

$$\begin{cases} \frac{d\phi_s}{dt} = V_{ds} - R_s I_{ds}, \\ T_e = \frac{P\phi_s}{R_s}\left(V_{qs} - \omega_a \phi_s\right). \end{cases} \tag{19}$$

Indeed, the DTC-SVM is based mainly on the stator flux oriented control (SFOC) and benefits from the use of two PI controllers, the first one is used for the torque control and the second one is used for the flux control. These controllers contribute within a closed loop to providing the reference stator voltages in the $(d-q)$ frame as shown in Fig.5. Then these obtained voltages are used as the input for the SVPWM technique to generate the different switching patterns [8].

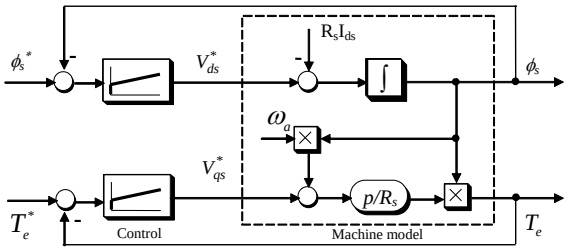

Figure 5: Block diagram of the flux and torque loops.

As shown in Fig.6(a), four active space vectors (two medium vectors and two large vectors) in each sector, will be applied for the production of the desired reference voltage at each sampling time step. Therefore, the main task of the SVPWM techniques is the determination of the times of application of each vector in each sector to synthesize the output voltage vector as required. The four times of application of the four vectors are nominated as $t_{al}, t_{bl}, t_{am}, t_{bm}$ [18]. These times are calculated based on the following equations and are shown in Fig.6(b).

$$t_a = \frac{\left|\bar{V}_s^*\right| \sin(k\pi/5 - \alpha)}{\left|\bar{V}_l\right| \sin(\pi/5)} t_s, \quad t_b = \frac{\left|\bar{V}_s^*\right| \sin(\alpha - (k-1)\pi/5)}{\left|\bar{V}_l\right| \sin(\pi/5)} t_s, \tag{20}$$

where k is the sector number (k= 1 to 10),

$$\begin{aligned} t_{al} &= \frac{\left|\bar{V}_l\right|}{\left|\bar{V}_l\right| + \left|\bar{V}_m\right|} t_a, \quad t_{am} = \frac{\left|\bar{V}_m\right|}{\left|\bar{V}_l\right| + \left|\bar{V}_m\right|} t_a, \\ t_{bl} &= \frac{\left|\bar{V}_l\right|}{\left|\bar{V}_l\right| + \left|\bar{V}_m\right|} t_b, \quad t_{bm} = \frac{\left|\bar{V}_m\right|}{\left|\bar{V}_l\right| + \left|\bar{V}_m\right|} t_b. \end{aligned} \tag{21}$$

The zero space vector application time is given by $t_0 = t_s - t_{al} - t_{am} - t_{bl} - t_{bm}$.

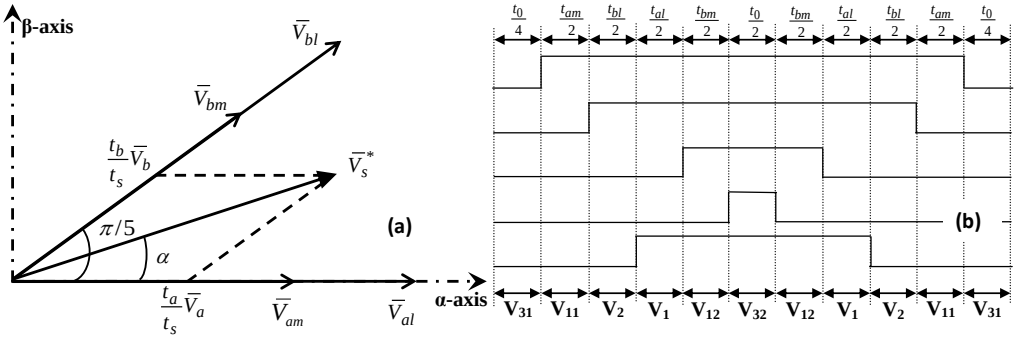

Figure 6: (a) Vector time calculation for the five-phase VSI in the first sector, (b) SVPWM switching pattern (the 1^{st} sector using large and medium space vector) [18].

4 Speed and Flux Full-Order Adaptive Observer

The stator and rotor equations of the five-phase IM model in the $\alpha-\beta$ stationary reference frame can be obtained by applying only the Clark transformation to equation (12). The new resulting ones can be written as follows:

$$\begin{cases} V_{\alpha s} = R_s I_{\alpha s} + p\phi_{\alpha s}, & V_{\beta s} = R_s I_{\beta s} + p\phi_{\beta s}, \\ 0 = R_r I_{\alpha r} + \omega\phi_{\beta r} + p\phi_{\alpha r}, & 0 = R_r I_{\beta r} - \omega\phi_{\alpha r} + p\phi_{\beta r}. \end{cases} \tag{22}$$

In the same manner, the magnetic equations of the stator and rotor flux can be rewritten as follows:

$$\begin{cases} \phi_{\alpha s} = L_s I_{\alpha s} + L_m I_{\alpha r}, & \phi_{\alpha r} = L_r I_{\alpha r} + L_m I_{\alpha s}, \\ \phi_{\beta s} = L_s I_{\beta s} + L_m I_{\beta r}, & \phi_{\beta r} = L_r I_{\beta r} + L_m I_{\beta s}. \end{cases} \tag{23}$$

The obtained model of the five-phase IM can be written further in the canonical space state form as follows:

$$\dot{X} = AX + BU, \tag{24}$$

where

$$X = [I_{\alpha s}, I_{\beta s}, \phi_{\alpha r}, \phi_{\beta r}]^T, \quad U = [V_{\alpha s}, V_{\beta s}], \tag{25}$$

$$A = \begin{bmatrix} a & 0 & b & bT_r\omega \\ 0 & a & -bT_r\omega & b \\ \frac{L_m}{T_r} & 0 & -\frac{1}{T_r} & -\omega \\ 0 & \frac{L_m}{T_r} & \omega & -\frac{1}{T_r} \end{bmatrix}, \quad B = \begin{bmatrix} \frac{1}{\sigma L_s} & 0 \\ 0 & \frac{1}{\sigma L_s} \\ 0 & 0 \\ 0 & 0 \end{bmatrix}, \tag{26}$$

$$a = -\frac{1}{\sigma L_s}\left(R_s + \frac{L_m^2}{L_r T_r}\right), \quad b = \frac{L_m}{\sigma L_s T_r L_r}, \quad \sigma = 1 - \frac{L_m^2}{L_s L_r}, \quad T_r = \frac{L_r}{R_r}. \tag{27}$$

A full-order observer is proposed and can be build based on the system of equations (24), where the rotor speed is supposed to be constant within each sampling period, which is considered in this work as an additional assumption to be taken into account. Furthermore, it is important to clarify that this assumption is very realistic and practical as the mechanical time constant is relatively larger compared to the electrical time constant. The operating model of the obtained full-order observer can be presented as follows [19]:

$$\dot{\hat{X}} = A\hat{X} + BU + G\left(\hat{I}_s - I_s\right), \tag{28}$$

$$\hat{A} = \begin{bmatrix} a & 0 & b & bT_r\hat{\omega} \\ 0 & a & -bT_r\hat{\omega} & b \\ \frac{L_m}{T_r} & 0 & -\frac{1}{T_r} & -\hat{\omega} \\ 0 & \frac{L_m}{T_r} & \hat{\omega} & -\frac{1}{T_r} \end{bmatrix}, \quad I_s = [I_{\alpha s}, I_{\beta s}]^T . \tag{29}$$

The symbol $(\hat{X})$ denotes the estimated values, G is the observer gain matrix, which is determined by the following equation such that the observer poles are proportional to those of the induction motor (the proportionality constant is k, and $k >= 1$) [19]:

$$G = \begin{bmatrix} g_1 & g_2 & g_3 & g_4 \\ -g_2 & g_1 & -g_4 & g_3 \end{bmatrix}, \tag{30}$$

where

$$\begin{aligned} &g_1 = (k-1)\,(a - 1/T_r)\,, \quad g_2 = (k-1)\hat{\omega}, \quad g_4 = -c(k-1)\hat{\omega}, \\ &g_3 = \left(k^2 - 1\right)(ca + L_m/T_r) - c(k-1)\,(a - 1/T_r)\,, \quad c = \tfrac{1}{bT_r}. \end{aligned} \tag{31}$$

By using (28) and (29), it is possible to implement a speed estimator, which is able to estimate the rotor speed in real time by using the adaptive state observer shown in Fig.7 [19].

$$\hat{\omega} = K_p \left(e_{i\alpha s}\hat{\phi}_{\beta r} - e_{i\beta s}\hat{\phi}_{\alpha r}\right) + K_i \int \left(e_{i\alpha s}\hat{\phi}_{\beta r} - e_{i\beta s}\hat{\phi}_{\alpha r}\right) dt, \tag{32}$$

where K_p and K_i are arbitrary positive gains.

$$e_{i\alpha s} = I_{\alpha s} - \hat{I}_{\alpha s} \quad \text{and} \quad e_{i\beta s} = I_{\beta s} - \hat{I}_{\beta s}. \tag{33}$$

In this observer, only d and q voltage components of the five-phase machine are used since d_1 and q_1 components do not present any significant contribution in the estimation.

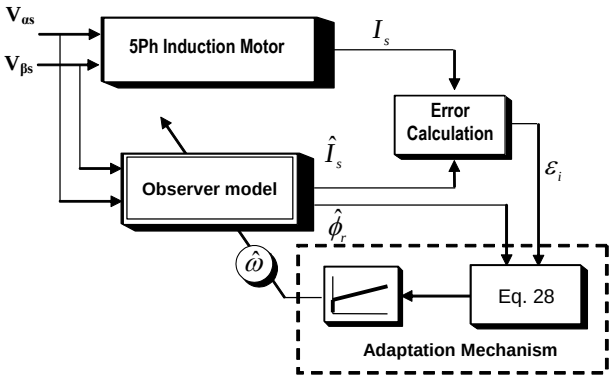

Figure 7: Block diagram of the adaptive flux and speed observer.

5 Model Reference Adaptative System MRAS

In this section, the model reference adaptive system technique (MRAS) is used to perform the sensorless direct torque control of the five-phase induction motor using the values resulting from the estimation of the rotor flux and the rotor speed based on the available

measurements of stator currents and voltages. Indeed, this technique possesses simple process of programming and implementation, where it benefits mainly from the advantage of using two decoupled models of the motor under study to ensure the estimation of the required states [15, 20]. The first estimation model called the reference model does not require the computation of the rotor speed, it is rotor speed independent, and it serves in the estimation of the rotor flux based on two inputs, that is, the measured stator current and the controlled stator voltage (measured or computed based on the SVPWM process) at the output side of the inverter. The second model is a tuning model which is called the adaptive (adjustable) model, it requires as an input only the stator measured current and uses the estimated rotor speed to adjust the output which is the adjustable rotor flux. A defined error between the two outputs of the aforementioned model will be used via a PI controller with a simple gain which performs the adaptation process of the proposed MRAS for obtaining the estimated rotor speed. It is worthy here to clarify that the MRAS process is based on the components of the stationary frame α-β.

Based on the equations of rotor flux in (15) and the equation of stator voltages in (14), the derivative of the rotor flux components can be written as follows:

$$\begin{cases} d\phi_{\alpha r}^{(1)}/dt = \frac{L_r}{L_m}\left(V_{\alpha s} - \left(R_s + \sigma L_s p\right) i_{\alpha s}\right), \\ d\phi_{\beta r}^{(1)}/dt = \frac{L_r}{L_m}\left(V_{\beta s} - \left(R_s + \sigma L_s p\right) i_{\beta s}\right), \end{cases} \tag{34}$$

where $\sigma = 1 - \frac{L_m^2}{L_s L_r}$.

This equation presents the first model, where it is clear that from the measured stator currents $(i_{\alpha s}, i_{\beta s})$ and the stator voltage components $(v_{\alpha s}, v_{\beta s})$ obtained from the output controlled inverter, the two components of the rotor flux $(\phi_{\alpha s}, \phi_{\beta s})$ can be calculated (estimated) as shown in Fig.8. Based on the equations of rotor flux in (15) and the equation of rotor voltages in (14), the derivative of the rotor flux components can be written as follows:

$$\begin{cases} d\phi_{\alpha r}^{(2)}/dt = -\frac{1}{T_r}\phi_{\alpha r}^{(2)} - \hat{\omega}_r \phi_{\beta r}^{(2)} + \frac{L_m}{T_r} i_{\alpha s}, \\ d\phi_{\beta r}^{(2)}/dt = -\frac{1}{T_r}\phi_{\beta r}^{(2)} + \hat{\omega}_r \phi_{\alpha r}^{(2)} + \frac{L_m}{T_r} i_{\beta s}, \end{cases} \tag{35}$$

where $T_r = \frac{L_r}{R_r}$.

This equation presents the second model, where it is clear that from only the measured stator currents $(i_{\alpha s}, i_{\beta s})$, the previous estimated rotor speed $(\hat{\omega}_r)$ at the MRAS output and the two previous estimated components of the adjustable rotor flux $(\phi_{\alpha s}, \phi_{\beta s})$, the actual two components of the estimated flux can be obtained as shown in Fig.8. The error which is used at the input of the PI controller is defined as follows:

$$e_\phi = \phi_{\beta r}^{(1)} \phi_{\alpha r}^{(2)} - \phi_{\alpha r}^{(1)} \phi_{\beta r}^{(2)}. \tag{36}$$

Finally, the estimated actual speed is obtained as follows:

$$\hat{\omega}_r = k_p e_\phi + k_i \int e_\phi. \tag{37}$$

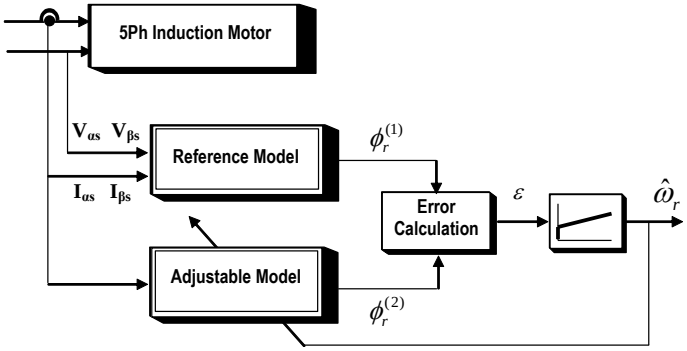

Figure 8: Block diagram of the MRAS speed estimator.

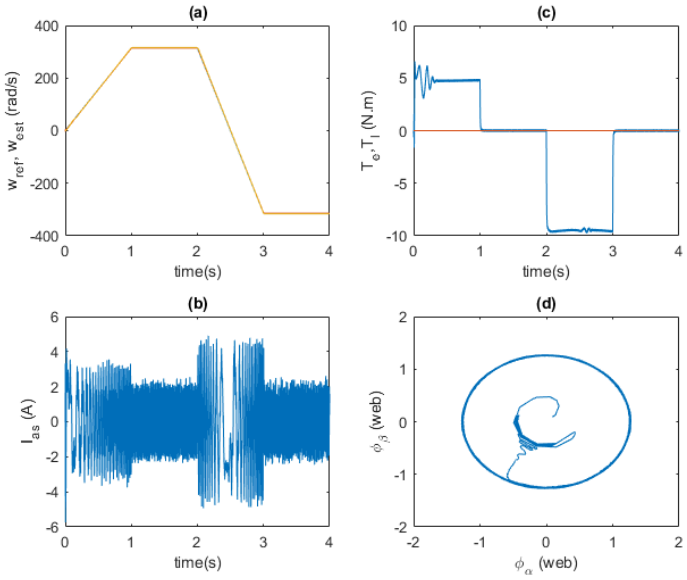

Figure 9: Adaptive observer (speed reverse condition): (a) reference speed, estimated speed, (b) stator current, (c) electromagnetic torque, (d) α and β axes stator fluxes versus each other.

6 Results

In this section, the two investigated speed estimation approaches in combination with the DTC-SVM, which have been presented in the previous sections to ensure the sensorless control of the five-phase induction machine, have been performed via simulation under MATLAB/Simulink. Indeed, the main aim of the presented simulation is the evaluation of the effectiveness and the performances of both approaches in ensuring the dynamic stability of the speed control of the machine being studied under two specific speed profiles within the rated speed range and low speed range.

In these simulations, a profile of the reference speed variation is proposed and contains

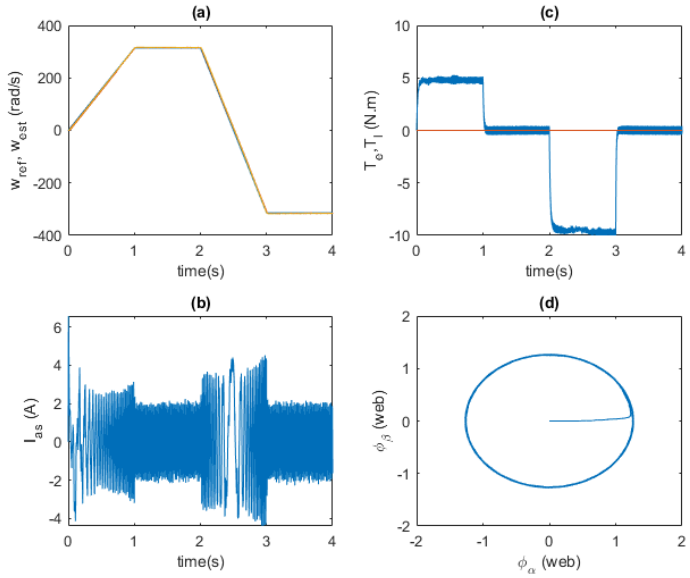

Figure 10: MRAS estimator (speed reverse condition): (a) reference speed, estimated speed, (b) stator current, (c) electromagnetic torque, (d) α and β axes stator fluxes versus each other.

the reverse of the speed direction as shown in Figs.9(a) and 10(a) under no-load torque application. The main characteristics of the five-phase induction motor used in these simulations are presented in Table 1.

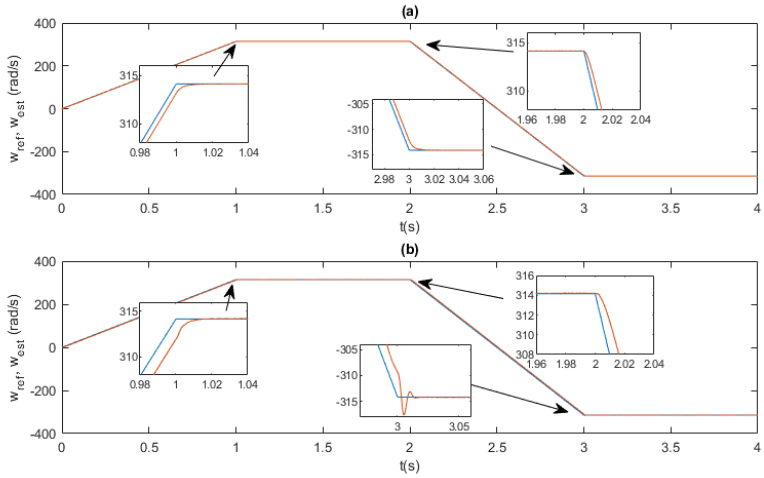

Figure 11: Zoom at the point of speed changes for (a) ASO and (b) MRAS.

It can be seen clearly from Fig.9(a) and Fig.10(a) that the reference of the rotor speed profile is the same for both approaches and it includes four main steps, two transient

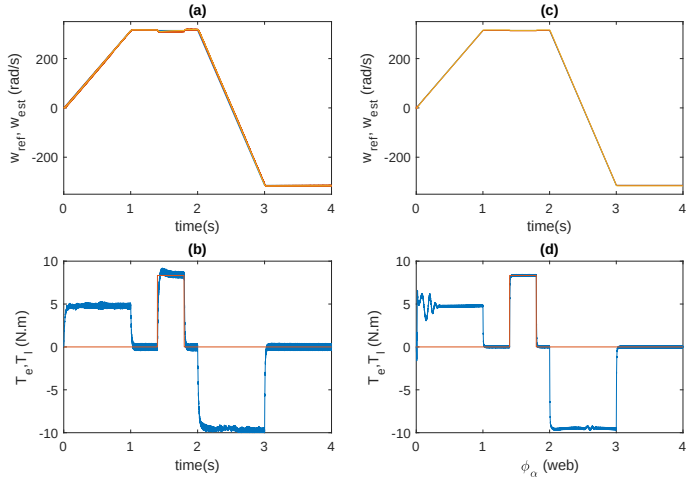

Figure 12: Under the load and speed reverse condition 1- MRAS estimator: (a) reference and estimated speed, (b) load and electromagnetic torque; 2- Adaptive observer: (c) reference and estimated speed, (d) load and electromagnetic torque.

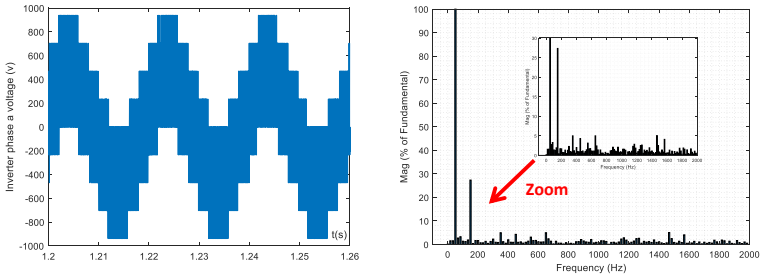

Figure 13: Harmonic Spectrum for output voltage using Adaptive Observer.

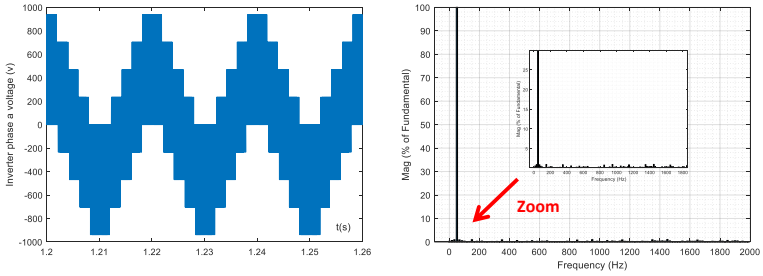

Figure 14: Harmonic Spectrum for output voltage using the MRAS estimator.

steps and two steady steps. The first step takes place from 0 s to 1 s, it is the start-up step which is a transient step in the forward direction, where the speed changes from 0 rad/s to its nominal rated speed 1500 rpm (314.15 rad/s electrical).

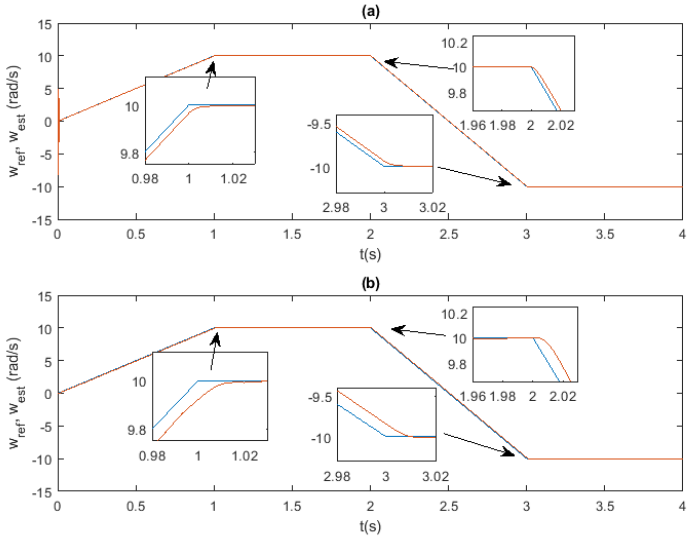

Figure 15: Speed reverse condition at low-speed operation: (a) Reference and estimated speed (ASO), (b) Reference and estimated speed (MRAS).

The second step takes place from 1 s to 2 s, it is a steady step where the speed is kept constant at its nominal rated value in the forward direction. The third step is the second transient step in which the speed changes from its nominal rated speed in the forward direction to the same value of speed but in the reverse direction (backward direction) within the interval of time from 2 s to 3 s. The last step is the second steady step, where the speed remains constant in the reverse direction at the nominal rated speed from 3 s to 4 s. It is obvious from Fig.9(a) and Fig.10(a) that in both cases of application of the adaptive speed observer (ASO) and the MRAS, respectively, the rotor speed of the five-phase induction motor follows accurately the reference speed profile with neglected errors within the two steady steps among the imposed four steps of the reference speed profile, while very small errors are noticed during the transient steps for both sensorless control approaches used.

Fig.9(b) and Fig.10(b) show the waveforms of the stator current of phase (a) for both approaches. It is clear that both currents follow the dynamics of the speed profile, where increased currents are noticed during the start-up and speed reverse due to the required electromagnetic torque developed by the induction motor in both cases.

Fig.9(c) and Fig.10(c) show the developed electromagnetic torque in both cases. It is obvious that within the start-up step in the case of MRAS approach, the developed torque reaches the required torque with neither remarkable overshoot nor oscillations. Meanwhile, in the case of ASO, a remarkable overshoot and oscillations can be noticed clearly, which presents a bit drawback compared to the MRAS approach. However, during other steps both approaches dynamics behave in the same way.

Fig.9(d) and Fig.10(d) present the β-axis flux function of the α-axis, where it can be seen clearly that it has a circular form in both cases with less oscillations due to neglected harmonics components in the flux components following both axes. On the other side, there is no observable impact of the variations of the speed, mainly during the transient

steps, which confirms the enhanced dynamics of both sensorless control approaches used, except the one observed during the start-up for the ASO approach which makes the curve in the flux plan reach the circle a bit later compared to the MRAS approach.

Fig.11 shows the zooms of three regions within the reference profile speed and the estimated rotor speed at the instant of their changes under both approaches of ASO and MRAS, respectively. It can be noticed clearly that the ASO has a little more accurate tracking of the reference speed compared to the MRAS. However, this difference is too limited and it does not affect the real dynamic of the motor in tracking the profile speed.

Fig.12 shows the rotor speed dynamics under the application of both sensorless control approaches with the same aforementioned reference speed profile as in the previous simulations, however, in this simulation a load torque, which is chosen to be equal to the rated nominal load torque of 8.33 N.m, is applied during the first steady step from 1.4 s to 1.8 s. As there is no change in the profile of the reference speed profile, the same dynamics is obtained in the regions where there is no load torque. Indeed, it can be noted that the rotor speed decreases lightly when the load torque is applied in the case of MRAS, and this decrease is neglected in the case of ASO.

Figs.13 and 14 present the waveforms and harmonic spectrums of the inverter output voltage of phase "a" applied to the five-phase induction motor, which are obtained by the application of the SVPWM technique under the ASO and MRAS approaches, respectively. It is clear that the low frequency harmonics have less values in the case of the MRAS approach compared to the ASO approach. This issue does not affect really the stator currents and the developed electromagnetic torque due to the fact that the inductance in each phase serves good enough as a low-pass filter for damping the current ripples and, consequently, the torque ripples. Hence, it can be said that the quality of both obtained voltages is acceptable in practical applications.

The last simulation is dedicated to the low-speed profile within a very limited range from -10 rad/s to 10 rad/s, which is shown in Fig.15. It can be observed that both approaches possess high dynamic performances in ensuring the tracking of the reference speed without failure during all step changes. Hence, it can be concluded that both approaches are valid in ensuring the sensorless control of the five-phase induction machine within a wide range of speed variation with a very little advantage of the MRAS compared to the ASO.

Rated voltage	$U_n = 220$ v	Stator Resistance	$R_s = 10\Omega$
Rated Current	$I_n = 2.1$ A	Rotor Resistance	$R_r = 6.3\Omega$
Stator inductance	$L_s = 0.46$ H	Mutual Inductance	$L_m = 0.42$ H
Rotor Inductance	$L_r = 0.46$ H	Number of poles pairs	$p = 2$
Moment of Inertia	$J = 0.03kg.m^2$	Friction coefficient	$f_r = 0.008$ N.m.s/rd

Table 1: The Parameters of the Five-Phase Induction Machine.

7 Conclusion

In this paper, the sensorless control of the five-phase induction motor using the direct torque control combined with space vector modulations (DTC-SVM) is presented and analyzed. Indeed, the main aim of the application of this control is to ensure the accurate

control of the rotor speed with improved dynamic performances following an imposed reference rotor speed profile which includes speed variation and direction inversion under torque load variation. This paper investigates the use of two different speed techniques for the estimation of the rotor speed used in the applied DTC-SVM, namely, the adaptive flux and speed observer and the model reference adaptive system (MRAS). Both sensorless control approaches are tested in this work based on the proposed profile of the rotor speed using simulation. The obtained results show that the application of both approaches has ensured the desired control performance and it can be said that their dynamic behaviors are the same as at their application to the three-phase induction machine. However, the analysis of the application of both estimation approaches shows that the sensorless control approach based on the MRAS has rather simple structure, easy implementation and requires less time of computation compared to the adaptive flux and speed observer, these features make the MRAS more advantageous in practical implementation and industrial applications for the sensorless control of the five-phase induction motor.

References

[1] Z. Liu, Y. Li and Z. Zheng. A review of drive techniques for multiphase machines. *CES Transactions on Electrical Machines and Systems* **2** (2) (2018) 243–251.

[2] I. Takahashi and T. Noguchi. A new quick response and high efficiency control strategy of an induction motor. *IEEE Trans. ind. Applicat.* **IA** (22) (1986) 820—827.

[3] M. Depenbrock. Direct self control of inverter-fed induction machines. *IEEE Trans. Power Electron.* **3** (1988) 420-–429.

[4] Y. Tatte and M. Aware. Direct Torque Control of Five-Phase Induction Motor with Common-Mode Voltage and Current Harmonics Reduction. *IEEE Transactions on Power Electronics* **32** (11) (2017) 8644–8654.

[5] Y. Chedni, DJ. Boudana, A. Moualdia, L. Nezli and P. Wira. Sensorless Two Series Connected Quasi Six-Phase IM Based Direct Torque Control for Torque Ripples Minimization. *Nonlinear Dynamics and Systems Theory* **20** (2) (2020) 153–167.

[6] T. Djellouli, S. Moulahoum, A. Moualdia, M. S. Bouchrit and P. Wira. Speed Sensorless Direct Torque Control Strategy of a Doubly Fed Induction Motor Using an ANN and an EKF. *Nonlinear Dynamics and Systems Theory* **20** (4) (2020) 374–387.

[7] H. Xu and H. A. Toliyat. A novel direct torque control (DTC) method for five-phase induction machines. In: *Proc. Applied Power Electron. Conf. Exp., APEC* **1** (2000) 162–168.

[8] Y. S. Lai and J. H. Chen. A new approach to direct torque control of induction motor drives for constant inverter switching frequency and torque ripple reduction. *IEEE Transactions on Energy Conversion* **16** (3) (2001) 220–227.

[9] B. S. Khaldi, H. Abu-Rub, A. Iqbal, R. Kennel, M. O. Mahmoudi and D. Boukhetala. Comparison study between a simple sensorless method and adaptive observer for DTC-SVM five-phase induction motor drive. *IEEE International Conference on Industrial Technology*, Athens, (2012) 743–748.

[10] H. Echeikh, R. Trabelsi, A. Iqbal, R. Alammari and M. F. Mimouni. Sensorless indirect rotor flux oriented control of a five-phase induction motor based on sliding mode observer. In: *International Conference on Sciences and Techniques of Automatic Control and Computer Engineering* (2015) 471–479.

[11] O. González, J. Rodas, R. Gregor, M. Ayala and M. Rivera. Speed sensorless predictive current control of a five-phase induction machine. In: *IEEE Conference on Industrial Electronics and Applications,* (2017) 343–348.

[12] M. Morawiec and F Wilczyński. Sensorless Control of Five-phase Machine Supplied by the Current Source Inverter. *International Conference on Electrical Power Drive Systems.,* (2020) 1-6.

[13] A. S. Morsy, A. S. Abdel-Khalik, S. Ahmed and A. Massoud. Sensorless V/f control with MRAS speed estimator for a five-phase induction machine under open-circuit phase faults. *7th IEEE GCC Conference and Exhibition,* Doha, (2013) 268–273.

[14] H. Abu-Rub, M. R. Khan, A. Iqbal and S. M. Ahmed. MRAS-based sensorless control of a five-phase induction motor drive with a predictive adaptive model. In: *IEEE International Symposium on Industrial Electronics,* Bari, (2010) 3089–3094.

[15] S. Khadar, A. Kouzou, A. Hafaifa and A. Iqbal. Investigation on SVM-Backstepping sensorless control of five-phase open-end winding induction motor based on model reference adaptive system and parameter estimation. *Engineering Science and Technology, an International Journal* **22** (4) (2019) 1013–1026.

[16] E. Levi, M. Jones, S. N. Vukosavic and H. A. Toliyat. A novel concept of a multiphase, multimotor vector controlled drive system supplied from a single voltage source inverter. *IEEE Trans. Power Electron.* **19** (2) (2004) 320–335.

[17] D. Casadei, F. Profumo, G. Serra and A. Tani. FOC and DTC: two viable schemes for induction motors torque control. *IEEE Trans. Power Electron.* **17** (5) (2002) 779–787.

[18] A. Iqbal and S Moinuddin. Comprehensive Relationship Between Carrier-Based PWM and Space Vector PWM in a Five-Phase VSI. *IEEE Trans. Power Electron.* **24** (10) (2009) 2379–2390.

[19] P. Vas. *Sensorless Vector and Direct Torque Control.* London: Oxford Univ. Press. 2003.

[20] A. Pal, S. Das and A. K. Chattopadhyay. An improved rotor flux space vector based MRAS for field-oriented control of induction motor drives. *IEEE Trans. Power Electron.* **33** (6) (2018) 5131–5141.